Title

A common polymorphism associated with antibiotic-induced cardiac arrhythmia

Journal
Proceedings of the National Academy of Sciences of the United States of America, 97(19)

ISSN
0027-8424

Authors
Sesti, Federico
Abbott, Geoffrey W
Wei, Jian
et al.

Publication Date
2000-09-12

DOI
10.1073/pnas.180223197

A common polymorphism associated with antibiotic-induced cardiac arrhythmia

Federico Sesti*, Geoffrey W. Abbott*, Jian Wei†, Katherine T. Murray†, Sanjeev Saksena‡, Peter J. Schwartz§, Silvia G. Priori§, Dan M. Roden†, Alfred L. George, Jr.†, and Steve A. N. Goldstein*¶

*Departments of Pediatrics and Cellular and Molecular Physiology, Boyer Center for Molecular Medicine, Yale University School of Medicine, New Haven, CT 06536; †Departments of Medicine and Pharmacology, Vanderbilt University, Nashville, TN 37235; ‡Robert Wood Johnson Medical School, Passaic, NJ 07055; and §Department of Cardiology, University of Pavia and Policlinico San Matteo IRCCS, Pavia, Italy 27100

Edited by Vincent T. Marchesi, Yale University School of Medicine, New Haven, CT, and approved July 6, 2000 (received for review May 16, 2000)

Drug-induced long QT syndrome (LQTS) is a prevalent disorder of uncertain etiology that predisposes to sudden death. *KCNE2* encodes MinK-related peptide 1 (MiRP1), a subunit of the cardiac potassium channel I_{Kr} that has been associated previously with inherited LQTS. Here, we examine *KCNE2* in 98 patients with drug-induced LQTS, identifying three individuals with sporadic mutations and a patient with sulfamethoxazole-associated LQTS who carried a single-nucleotide polymorphism (SNP) found in ≈1.6% of the general population. While mutant channels showed diminished potassium flux at baseline and wild-type drug sensitivity, channels with the SNP were normal at baseline but inhibited by sulfamethoxazole at therapeutic levels that did not affect wild-type channels. We conclude that allelic variants of MiRP1 contribute to a significant fraction of cases of drug-induced LQTS through multiple mechanisms and that common sequence variations that increase the risk of life-threatening drug reactions can be clinically silent before drug exposure.

MiRP1 | LQTS | SNP | Bactrim | sulfamethoxazole

Inherited long QT syndrome (LQTS) is an uncommon cardiac arrhythmia that predisposes to *torsades de pointes* (TdP), ventricular fibrillation, and sudden death (1–4). The molecular basis for LQTS is known: delayed repolarization of the myocardium prolongs the cardiac action potential increasing the QT interval measured on the surface electrocardiogram. Mutations in five ion channel genes cause the majority of cases of inherited LQTS. LQTS mutations in *SCN5A* increase activity of the sodium channel that depolarizes the myocardium to initiate the cardiac action potential (5); LQTS mutations in *KCNE1* or *KvLQT1* (encoding subunits of I_{Ks} channels) and *KCNE2* or *HERG* (encoding subunits of I_{Kr} channels) diminish potassium fluxes that repolarize the heart to end each beat (6–9).

Acquired LQTS is a common disorder caused by drugs and metabolic abnormalities. The risk for acquired LQTS increases when factors that decrease potassium flux act concurrently to impair the ability of the myocardium to repolarize. Well-recognized conditions that diminish "repolarization reserve" include female gender, hypokalemia, and drugs that inhibit cardiac potassium channels (10). Several lines of evidence suggest that patients with drug-induced LQTS have an underlying predisposition to dysrrhythmia. The QT interval measured before drug exposure tends to be longer in patients who later develop drug-induced LQTS than in individuals who receive the same agent safely (11, 12). Moreover, sporadic mutations have been identified in patients with drug-induced TdP (9, 13, 14). Thus, we demonstrated previously that patients with "acquired" LQTS can have a genetic predisposition to arrhythmia because of mutation in the MinK-related peptide 1 (MiRP1) subunit of their I_{Kr} potassium channels (9). In that study, a woman with clarithromycin-induced TdP was found to carry a sporadic missense mutation in *KCNE2*; channels formed with the altered subunit (Q9E-MiRP1) were abnormal at baseline because they activated less readily (and so passed less potassium); moreover, Q9E-MiRP1 channels were 3-fold more sensitive to drug inhibition than wild type. In that case, a rare mutation increased the risk of drug-induced TdP by both decreasing repolarization reserve and increasing sensitivity to an agent that is usually well tolerated.

Here we examine *KCNE2* in 98 patients with drug-induced arrhythmia and identify four missense variants, three mutations that diminish potassium flux at baseline (M54T-, I57T- and A116V-MiRP1) and a single-nucleotide polymorphism (SNP) producing T8A-MiRP1 that is present in ≈1.6% of healthy individuals (9). Our patient with the SNP had a normal electrocardiogram at rest but developed a very long QT interval on Bactrim [trimethoprim/sulfamethoxazole (TMP/SMX)] therapy. The apparent etiology: channels formed with T8A-MiRP1 are inhibited by SMX at levels present in the sera of patients on TMP/SMX.

Materials and Methods

Study Subjects. The female/male ratio in this study population was 2:1, and 95 patients were Caucasian. Informed consent was obtained from each subject approved by the Vanderbilt University Institutional Review Board.

Mutation Analysis. The GenBank accession number for human *KCNE2* encoding MiRP1 is AF071002. Genomic DNA was isolated from peripheral blood leukocytes by standard methods and two overlapping regions of the *KCNE2* coding sequence screened for the presence of nucleotide sequence polymorphism by single-strand conformational polymorphism (SSCP) analysis (15). Oligonucleotide primer pairs used to amplify the *KCNE2* coding sequence were: section I (nucleotides 32–259 of accession no. AF071002), forward primer: 5′-TGT TCG CCT ATT TTA TTA TTT-3′; reverse primer: 5′-AAA GAG AAC ATT CCA ATC AT-3′; section II (corresponding to nucleotides 212-471), forward primer: 5′-TAC TAT GTC ATC CTG TAC CTC-3′; reverse primer: 5′-GTT AGC TTG GTG CCT TTC T-3′. Amplification reactions were carried out by using 200 ng genomic DNA, 0.5 μM primers, 0.2 mM deoxynucleotide triphosphates, and *Taq* polymerase. SSCP analysis was performed on 0.5× mutation detection electrophoresis (MDE) gels subjected to overnight electrophoresis at 4 W and stained with silver nitrate. Abnormal conformers were excised from dried gels, eluted into sterile water at room temperature, reamplified

This paper was submitted directly (Track II) to the PNAS office.

Abbreviations: LQTS, long QT syndrome; MiRP1, MinK-related peptide 1; SNP, single-nucleotide polymorphism; TdP, torsades de pointes; TMP/SMX, trimethoprim/sulfamethoxazole; CHO, Chinese hamster ovary.

¶To whom reprints should be addressed at: Yale University, BCMM, 295 Congress Avenue, New Haven, CT 06536. E-mail: steve.goldstein@yale.edu.

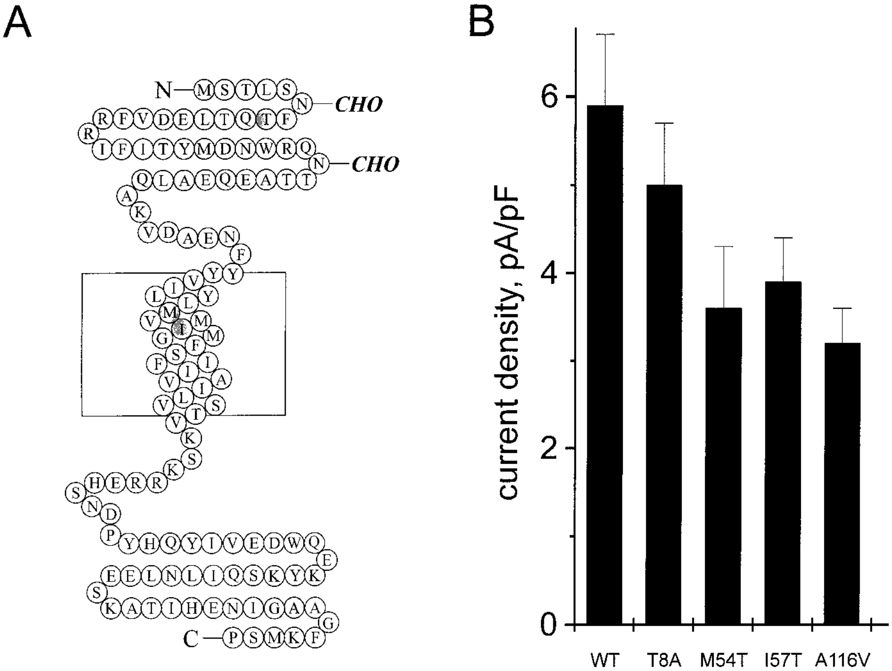

Fig. 1. KCNE2 missense mutations diminish I_{Kr} current density. (*A*) *KCNE2* polymorphisms identified in patients with acquired LQTS. Schematic of the predicted primary sequence and membrane topology of human MiRP1: a single transmembrane segment is based on the predicted sequence of MiRP1and its homology to MinK; an externally-oriented amino-terminal domain is based on antibody localization (9). Residues that were altered in patients in this study are indicated. (*B*) Current density assessed by normalizing steady-state tail currents at −40 mV to the cell capacitance for CHO cells expressing the indicated MiRP1 variants and HERG and studied by the standard protocol (*Materials and Methods*). Each bar represents the mean ± SEM for a group of 34–40 cells; the mean decrease in current density compared with wild-type MiRP1 was 15, 39, 34, and 47% for T8A-MiRP1, M54T-MiRP1, I57T-, and A116V-MiRP1, respectively, with $P < 10^{-4}$ for each variant compared with wild type (unpaired *t* test).

by using the original primers, and sequenced by using dye terminator chemistry. The presence of the *KCNE2*-A116V mutation was confirmed independently on PCR amplified genomic DNA by using an allele-specific hybridization assay with a ^{32}P end-labeled primer: 5′-AAC ATT GGT GTG GCT GGG TT-3′.

Heterologous Expression. Mutations identified in patients were produced in wild-type human *KCNE2* in pGA1 (9) by plaque-forming unit-based mutagenesis (QuickChange Kit; Stratagene, La Jolla, CA) followed by insertion of mutant gene fragments into translationally silent restriction sites in the wild-type construct and confirmed by automated DNA sequencing. Transient transfection of Chinese hamster ovary (CHO) cells was by DEA-Dextran, Chloroquine, and DMSO shock with *KCNE2* and *HERG* (Human ether a-go-go related gene) in pCl-neo-based vectors (Invitrogen) as before (9).

Electrophysiology. Data were recorded by using an Axopatch 200 B amplifier (Axon Instruments, Foster City, CA), a Quadra 800 Macintosh computer and PULSE software (Heka Electronics, Lombrecht/Pfalz, Germany). Sampled at 1 kHz, data are presented as mean ± SEM. All experiments were performed at room temperature. Holding voltage was −80 mV. Standard voltage protocol: 1-s prepulse from −60 to 20 mV in 10-mV step followed by 2-s step to −40 mV with a 1-s interpulse interval. Simulated cardiac action potential protocol: voltage ramp from 40 to −80 mV with a rate of change of −71 mV per second. Data are presented after ohmic leak subtraction (standard protocol) or subtraction of residual current after full drug block (simulated action potential). If leak was greater than 25% of total current, cells were discarded. The bath solution was (in mM): 100 NaCl/4 KCl/1 $CaCl_2$/0.7 $MgCl_2$/10 Hepes, pH 7.5 with NaOH. The pipette solution was (in mM): 100 KCl/10 Hepes/1 $MgCl_2$/2 EGTA, pH 7.5 with KOH. Stock solutions of oxatomide (Jensen, Spring House, PA), quinidine (Sigma), and procainamide (Sigma) were prepared by dissolution in bath solution at concentrations of 0.01, 1, and 10 mM, respectively. Oxatomide solution was prepared fresh daily. Sulfamethoxazole and trimethoprim (Sigma) are poorly soluble in water and were dissolved in ethanol at 100 mM or methanol at 20 mM, respectively. Solutions were then prepared daily by diluting stocks in bath solution. Sulfamethoxazole and trimethoprim were mixed 1:5 by weight as in TMP/SMX; control solutions for these studies were supplemented with equal levels of ethanol and/or methanol.

Results and Discussion

To examine the basis for drug-induced LQTS, genomic DNA samples were obtained from 98 patients who experienced excessive prolongation of the QT interval (>600 msec) or who developed TdP during drug treatment (see *Materials and Methods*). As *KCNE2* consists of a single coding exon (encoding a peptide of just 123 amino acids), it was amplified readily in two overlapping segments from genomic DNA, allowing the coding region to be screened for sequence polymorphism (*Materials and Methods*). Three sporadic mutations and one common polymorphism were found in four patients in our population. Mutations were identified that encoded M54T-, I57T-, and A116V-MiRP1; the first two were previously identified in patients with sporadic LQTS (9). One patient carried a polymorphism producing T8A-MiRP1, a *KCNE2* variant seen previously in 16 of 1,010 control individuals (9). The positions of these residues relative to the cell membrane are indicated on a schematic rendition of the predicted topology of MiRP1 (16) (Fig. 1*A*).

The *KCNE2* mutation that substituted threonine for methionine at amino acid 54 (M54T) was found in a patient who presented with procainamide-induced LQTS. This mutation was

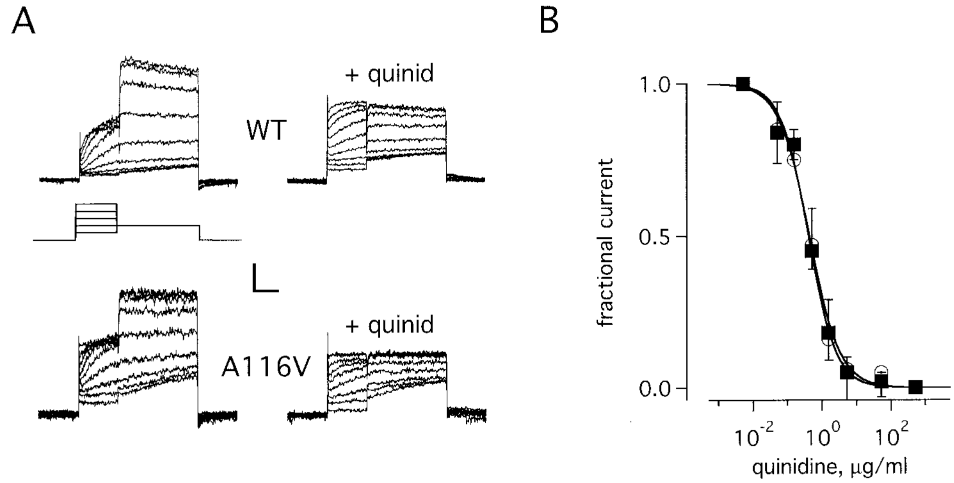

Fig. 2. I_{Kr} channels formed with A116V-MiRP1 show wild-type blockade by quinidine. CHO cells expressing wild-type MiRP1 or A116V-MiRP1 and HERG were studied by whole-cell clamp. (*A*) Whole-cell currents recorded from channels formed with wild-type MiRP1 (WT) and A116V-MiRP1 (A116V) in the absence (left column) or presence of 0.5 μg/ml of quinidine (+quinid). Scale bars represent 50 and 30 pA and 0.7 s for wild type and A116V-MiRP1, respectively. (*Inset*) Protocol: holding −80-mV, 1-s pulses from −60 to 20 mV in 10-mV steps, 2 s at −40 mV, 1-s interpulse interval. (*B*) Current–dose relationship for channels formed with wild-type MiRP1 (open circles) and A116V-MiRP1 (filled squares) in the presence of increasing amounts of quinidine. Data from peak currents at −40 mV after a prepulse to +20 mV by using the standard protocol. Theoretical lines were constructed to the function: $1/(1 + H)$ were $H = ([drug]/K_i)^n$. K_i and n represent the equilibrium dissociation constant and the Hill coefficient, respectively. Fits give values for K_i and n of 0.41 ± 0.04 μg/ml and 1.1 ± 0.1 for wild-type MiRP1 and 0.43 ± 0.06 μg/ml and 1.1 ± 0.2 for A116V-MiRP1; 6 cells in each case.

seen once before among 230 patients with sporadic LQTS but not in 1,010 controls (9); the antiarrhythmic medication procainamide has been associated with acquired LQTS previously (1).

The missense mutation that substituted a threonine for isoleucine at residue 57 (I57T) was found in a patient with a prolonged QT interval induced by the histamine H1 receptor antagonist oxatomide. This mutation was seen once before among 230 patients with sporadic LQTS (9); oxatomide has not been associated previously with dysrrhythmia.

A novel missense mutation substituting valine for alanine at position 116 (A116V) was found in a 55-year-old white female with a history of cardiac arrest associated with cocaine and alcohol abuse. Subsequent treatment with quinidine and mexiletine was tolerated for 6 years. After mexiletine was discontinued, she had syncope with TdP while on quinidine alone. Evaluation at that time also revealed new-onset heart failure. Sequence analysis revealed a C-to-T transition that was not detected in 1,010 control individuals evaluated previously (9) or in 200 control genes assessed in this study by an allele-specific hybridization assay. The antiarrhythmic quinidine has been associated with acquired LQTS (1).

A fourth missense variant was identified in a 45-year-old white male with a history of Marfan syndrome who had a normal QT interval at baseline but developed marked QT prolongation after three oral doses of TMP/SMX for treatment of a minor infection. Screening revealed a polymorphism that substituted alanine for threonine at MiRP1 position 8 (T8A). This *KCNE2* polymorphism was previously seen in 16 of 1,010 control individuals, 1 of 230 patients with sporadic LQTS, and 1 patient with quinidine-induced dysrrhythmia among 20 individuals with drug-induced arrhythmia (9).

To investigate the effects of changes in *KCNE2* on channel function, the properties of wild-type and mutant MiRP1/HERG channels were studied by transient expression in CHO cells in whole-cell patch-clamp configuration, as described before (*Materials and Methods*) (9). The three sporadic mutations (M54T-, I57T- and A116V-MiRP1) produced reductions of 34–47% in current density at −40 mV (that is, whole-cell current divided by membrane capacitance to normalize for cell size), whereas only a 15% decrease was observed with T8A-MiRP1 (Fig. 1*B*). This was compatible with our prior study showing that channels with M54T-MiRP1 activated less readily and deactivated more rapidly than channels formed with either wild type or T8A-MiRP1 (9). Consistent with these observations, patients carrying M54T-MiRP1 showed slightly prolonged QT intervals in the drug-free state, whereas the patient with T8A-MiRP1, like 17/18 individuals with this genotype studied previously (9), had a normal QT interval at baseline.

The three sporadic mutations identified in our patients with drug-induced LQTS did not alter sensitivity to drug inhibition. Fig. 2*A* shows currents carried by channels formed with wild-type MiRP1 or A116V-MiRP1 in the absence and presence of quinidine; the two channels showed the same sensitivity to equilibrium blockade (Fig. 2*B*). Similarly, channels with wild-type MiRP1 or M54T-MiRP1 showed the same sensitivity to procainamide (with equilibrium inhibition constants, K_i, of 190 ± 30 and 185 ± 35 μg/ml, $n = 6$, respectively), and those with wild-type MiRP1 and I57T-MiRP1 had the same sensitivity to oxatomide ($K_i = 0.18 \pm 0.05$ and 0.18 ± 0.04 μg/ml, $n = 5$, respectively). Of note, levels of quinidine and oxatomide that achieved half-maximal inhibition of channels in experimental cells were close to their therapeutic concentrations in the plasma of patients (17, 18). In contrast, procainamide and its principle metabolite *N*-acetylprocainamide achieved half-maximal blockade at levels over 50-fold higher than those found in plasma (19); the metabolite was even less potent than the parent compound ($K_i = 400 \pm 60$ and 390 ± 70 μg/ml for wild-type MiRP1 and M54T-MiRP1, $n = 5$, respectively). This suggests the proarrhythmic effects of procainimide may not be mediated by I_{Kr} channels.

Wild-type and T8A-MiRP1 channels were studied with TMP/SMX, as this agent was associated with a prolonged QT interval in our patient (Fig. 3). Although both channel types were blocked, those with T8A-MiRP1 were ≈2-fold more sensitive to TMP/SMX (Fig. 3*A*). Each active compound, TMP and SMX, was

PHYSIOLOGY

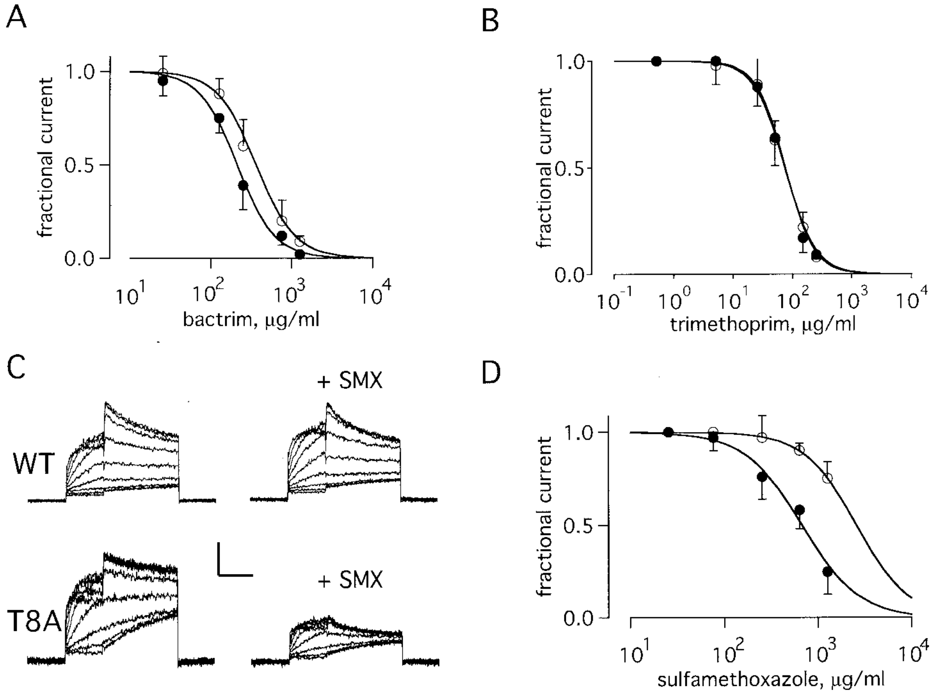

Fig. 3. Channels formed with T8A-MiRP1 are more sensitive to SMX. Currents and fits as in Fig. 2. (*A*) Current–dose relationship for channels formed with wild-type MiRP1 (open circles) and T8A-MiRP1 (filled circles) in the presence of increasing amounts of TMP/SMX. Data from peak currents at −40 mV after a prepulse to +20 mV by using the standard protocol. Fits give values for wild-type MiRP1 of K_i = 380 ± 40 μg/ml and n = 1.8 ± 0.3 and for T8A-MiRP1 of K_i = 210 ± 30 μg/ml and n = 1.9 ± 0.2; 13 cells in each case. (*B*) Current–dose relationships in the presence of TMP for wild-type MiRP1 (open circles) and T8A-MiRP1 (filled circles). Fits give values for K_i and n of 71 ± 12 μg/ml and 1.8 ± 0.4 for wild-type MiRP1 and 75 ± 9 μg/ml and 1.9 ± 0.3 for T8A-MiRP1; 5 cells each case. The data thus suggest inhibition was cooperative and two TMP molecules were required to block. (*C*) Whole-cell currents recorded from channels formed with wild-type MiRP1 (WT) and T8A-MiRP1 (T8A) in the absence (left column) or presence of 633 μg/ml of SMX (+SMX). Scale bars represent 50 pA and 40 pA for wild type and T8A, respectively, and 1 s. (*D*) Current–dose relationships in the presence of SMX for wild-type MiRP1 (open circles) and T8A-MiRP1 (filled circles). Fits give values for K_i and n of 2,600 ± 200 μg/ml and 1.6 ± 0.6 for wild-type MiRP1 and 675 ± 60 μg/ml and 1.4 ± 0.2 for T8A-MiRP1; 6 cells each case.

then investigated separately. Fig. 3*B* shows that TMP inhibited both channels with similar affinity ($K_i \approx 75$ μg/ml); a level of the agent far in excess of its usual plasma level, ≈5 μg/ml (20, 21). In contrast, SMX (633 μg/ml) had almost no effect on wild-type channels but inhibited more than half the flux through channels formed with T8A-MiRP1 at −40 mV (Fig. 3*C*). Channels with T8A-MiRP1 were at least 4-fold more sensitive to SMX than wild type (Fig. 3*D*). It seems reasonable to ascribe the proarrhythmic effects of Bactrim in our patient to its SMX component as serum levels for this agent can exceed 300 μg/ml (20, 21).

A notable difference in the effect of SMX on channels formed with T8A-MiRP1 and wild-type MiRP1 was apparent when gating kinetics were evaluated; the drug speeded deactivation (closure) only of channels with the SNP (Table 1). Thus, SMX increased both the fast and slow deactivation time constants for T8A-MiRP1 channels (enhancing τ_{fast} and τ_{slow} ≈4- and 2-fold, respectively) but had no significant effect on wild-type channels. As shown before (9), channels with the SNP showed a small shift in their half-maximal activation voltage ($V_{1/2}$) but no change in slope factor (V_s) compared with wild type (Table 1); SMX had no significant effect on the $V_{1/2}$ or V_s of either channel (Table 1).

To approximate the *in vivo* case with experimental cells, we used a voltage protocol that mimics a cardiac action potential (22) in the presence of physiological levels of drugs associated with LQTS in our patients. Flux of potassium across the membrane in each cycle was estimated from the area under the current curve. Fig. 4*A* shows raw traces of currents passed by wild-type MiRP1 or A116V-MiRP1 channels in the absence and presence of 0.5 μg/ml quinidine. At baseline, the mutant channels pass 46 ± 6% less potassium than wild type (n = 5). The two channel types were similarly sensitive to

Table 1. Gating parameters for wild-type (WT)- and T8A-MiRP1-containing channels

Channel (no. of cells)	Activation $V_{1/2}$, mV	Activation slope, mV	Deactivation τ_{fast}, s	Deactivation τ_{slow}, s	Deactivation ratio $I_{fast}/(I_{fast}+I_{slow})$
WT (10)					
Control	−20 ± 5	9.5 ± 1.4	0.4 ± 0.1	1.5 ± 0.4	0.5 ± 0.1
SMX	−20 ± 6	9.8 ± 2.2	0.3 ± 0.1	1.4 ± 0.3	0.5 ± 0.2
T8A (10)					
Control	−25 ± 6	9.0 ± 1.2	0.6 ± 0.2	1.4 ± 0.4	0.5 ± 0.1
SMX	−21 ± 5	9.4 ± 2.1	0.15 ± 0.04	0.9 ± 0.3	0.5 ± 0.1

Activation and deactivation kinetics were estimated in whole-cell recordings in the absence and presence of 633 μg/ml SMX. By using the protocol in Fig. 2, peak-tail currents at −40 mV were normalized and fit to the Boltzmann function: $1/\{1+\exp[(V_{1/2}-V)/V_S]\}$, where $V_{1/2}$ is half-maximal voltage and V_S the slope factor in mV. Deactivation kinetics were fit to a double exponential function ($I_0 + I_f e^{(-t/\tau f)} + I_s e^{(-t/\tau S)}$) at −40 mV after a prepulse to 20 mV as in Fig. 3.

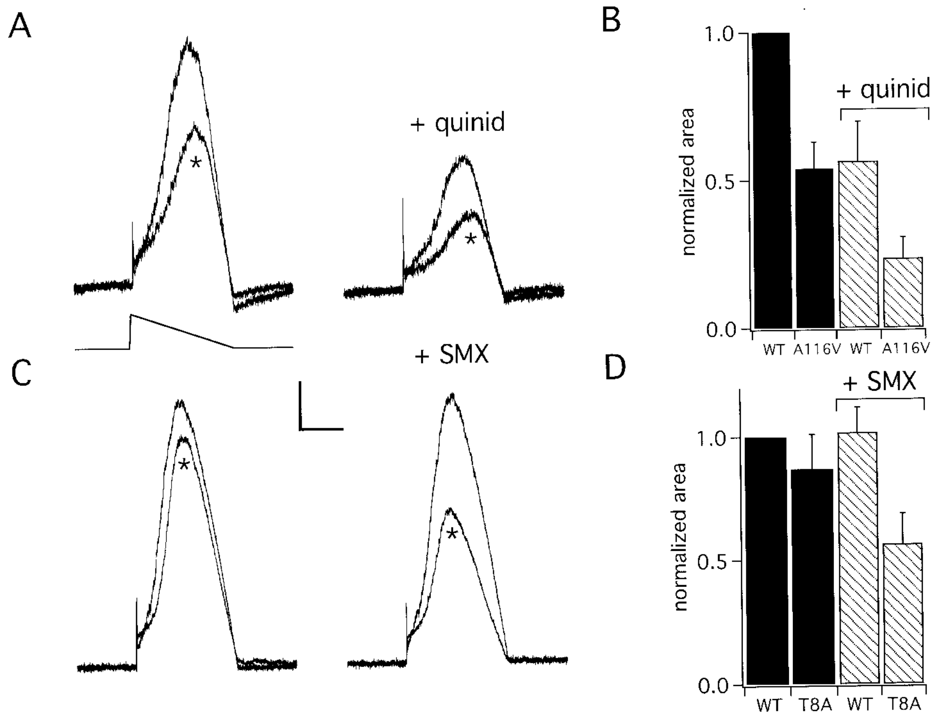

Fig. 4. Missense mutations and drug inhibition combine to diminish potassium flux. Simulated cardiac action potentials were used to study channels formed with wild-type MiRP1, A116V-MiRP1 and T8A-MiRP1 with HERG in CHO cells. (*A*) Whole-cell currents for simulated action potentials with wild-type MiRP1 and A116V-MiRP1 (*) in the absence and presence of 0.5 μg/ml quinidine (+quinid). Scale bars represent 1.3 pA/pF and 0.8 s. (*Inset*) Protocol: holding −80 mV, voltage ramp from 40 to −80 mV, dV/dt = −71 mV/s. (*B*) Normalized potassium flux assessed by measurement of area under the curve for simulated action potentials in cells expressing wild-type MiRP1 (WT) or A116V-MiRP1 (A116V) in the presence of 0.5 μg/ml quinidine (+quinid) normalized to wild-type channels without drug. Currents were divided by cell capacitance before normalization. Each bar represents the mean ± SEM for 6–10 cells. (*C*) Whole-cell currents for simulated action potentials with wild-type MiRP1 and T8A-MiRP1 (*) in the absence and presence of 300 μg/ml SMX. Scale bars represent 1.6 pA/pF and 0.8 s. (*D*) Normalized potassium flux assessed by measurement of area under the curve for simulated action potentials in cells expressing wild-type MiRP1(WT) and T8A-MiRP1 (T8A) in the presence of 300 μg/ml SMX normalized to wild-type channels without drug. Currents were divided by cell capacitance before normalization. Each bar represents the mean ± SEM for 7–10 cells.

drug inhibition showing ≈50% block at this drug dose. Therefore, with drug, A116V-MiRP1 channels passed ≈1/4 of the current carried by unblocked wild-type channels. These findings support the notion that A116V-MiRP1 decreased the ability of the myocardium to repolarize at baseline, placing our patient at increased risk for drug-induced arrhythmia when exposed subsequently to quinidine at therapeutic levels. We suggest superimposed heart failure further reduced repolarization reserve to increase the likelihood of TdP (23).

Figs. 4*C* shows raw traces of currents passed by wild-type MiRP1 and T8A-MiRP1 channels in the absence and presence of 300 μg/ml SMX. In the absence of drug, channels formed with the T8A-MiRP1 were largely indistinguishable from wild type, as expected (Table 1) (9). Although SMX at this dose did not significantly affect wild-type channels, current through T8A-MiRP1 channels was reduced to half the wild-type level (Fig. 4*D*; n = 5). Concordant with the observation that SMX speeds deactivation of T8A-MiRP1 channels, peak current was reached more rapidly in the presence of the drug (Fig. 4*C*), presumably because of increased channel availability, as with a disease-associated mutation of HERG that speeds deactivation (22).

These findings may explain why most patients receive TMP/SMX without incident (24) and others develop QT prolongation and TdP (25, 26). Although the large majority of individuals carry *KCNE2* genes encoding wild-type MiRP1, T8A-MiRP1 appears to predispose to arrhythmia by increasing the inhibitory effects of SMX, in part by speeding deactivation, placing 1–2% of the population at increased risk for SMX-induced arrhythmia.

Diseases caused by defects in single genes are rare (27). More common disorders such as diabetes (28), breast cancer (29), or hypertension (30) are thought to be caused by the combined influence of multiple susceptibility genes. So, too, the response of individual patients to drug therapy is expected to be influenced by genomic variation, for example, because of differences in drug metabolism or the structure or function of drug receptor molecules. The most common type of DNA sequence variation, SNPs, are observed at a frequency of ≈1/500–1,000 nucleotides in humans (31), and large-scale screening for SNPs (32) is now under way to advance efforts to identify disease susceptibility genes or to predict the response of individuals to drug therapies (33). Previous studies have indicated that a prolonged QT interval on a baseline electrocardiogram identifies individuals at increased risk for drug-induced arrhythmia, especially when administered medications that block cardiac potassium channels (9, 11). This study argues for the value of a "pharmacogenetic" approach to drug treatment, because it demonstrates that common sequence variations can be clinically silent before drug exposure yet increase the risk for life-threatening drug reactions. With further identification of allelic variants that increase susceptibility to cardiac arrhythmia, preprescription genotyping becomes a consideration.

This work was supported by grants from the National Institutes of Health (S.A.N.G., D.M.R., and A.L.G.). A.L.G. is an Established Investigator of the American Heart Association. We are grateful to N. Goldstein for support with graphics.

PHYSIOLOGY

1. Roden, D. M., Lazzara, R., Rosen, M., Schwartz, P. J., Towbin, J. & Vincent, G. M. (1996) *Circulation* **94,** 1996–2012.
2. Ackerman, M. J. & Clapham, D. E. (1997) *N. Engl. J. Med.* **336,** 1575–1586.
3. Keating, M. T. & Sanguinetti, M. C. (1996) *Science* **272,** 681–685.
4. Schwartz, P. J., Priori, S. G. & Napolitano, C. (2000) in *Cardiac Electrophysiology: From Cell to Bedside*, eds. Zipes, D. P. Jalife, J. (Saunders, Philadelphia), pp. 597–615.
5. Bennett, P. B., Yazawa, K., Makita, N. & George, A. L., Jr. (1995) *Nature (London)* **376,** 683–685.
6. Curran, M. E., Splawski, I., Timothy, K. W., Vincent, G. M., Green, E. D. & Keating, M. T. (1995) *Cell* **80,** 795–803.
7. Wang, Q., Curran, M. E., Splawski, I., Burn, T. C., Millholland, J. M., VanRaay, T. J., Shen, J., Timothy, K. W., Vincent, G. M., de Jager, T., *et al.* (1996) *Nat. Genet.* **12,** 17–23.
8. Splawski, I., Tristani-Firouzi, M., Lehmann, , M. H., Sanguinetti, M. C. & Keating, M. T. (1997) *Nat. Genet.* **17,** 338–340.
9. Abbott, G. W., Sesti, F., Splawski, I., Buck, M., Lehmann, M. H., Timothy, K. W., Keating, M. T. & Goldstein, S. A. N. (1999) *Cell* **97,** 175–187.
10. Roden, D. M. (1998) *Pacing Clin. Electrophysiol.* **21,** 1029–1034.
11. Roden, D. M. (1998) *Am. J. Cardiol.* **82,** 49I–57I.
12. Minardo, J. D., Heger, J. J., Miles, W. M., Zipes, D. P. & Prystowsky, E. N. (1988) *N. Engl. J. Med.* **319,** 257–262.
13. Donger, C., Denjoy, I., Berthet, M., Neyroud, N., Cruaud, C., Bennaceur, M., Chivoret, G., Schwartz, K., Coumel, P. & Gulcheney P. (1997) *Circulation* **96,** 2778–2781.
14. Napolitano, C., Schwartz, P. J., Brown, A. M., Ronchetti, E., Bianchi, L., Pinnovala, A., Acquaro, G. & Priori, S. G. (2000) *J. Cardiovasc. Electrophysiol.* **11,** 691–696.
15. Orita, M., Iwahana, H., Kanazawa, H., Hayashi, K. & Sekiya, T. (1989) *Proc. Natl. Acad. Sci. USA* **86,** 2766–2770.
16. Abbott, G. W. & Goldstein, S. A. N. (1998) *Quart. Rev. Biophys.* **31,** 357–398.
17. Davies, B. H. & Rocchiccioli, K. (1983) *Pharmatherapeutica* **3,** 365–369.
18. Kates, R. E. (1983) *Am. J. Cardiol.* **52,** 8C–13C.
19. Zema, M. J. & Mirando, T. (1983) *Angiology* **34,** 32–39.
20. Blaser, J., Joos, B., Opravil, M. & Luthy, R. (1993) *Infection* **21,** 206–209.
21. Joos, B., Blaser, J., Opravil, M., Chave, J. P. & Luthy, R. (1995) *Antimicrob. Agents Chemother.* **39,** 2661–2666.
22. Chen, J., Zou, A., Splawski, I., Keating, M. T. & Sanguinetti, M. C. (1999) *J. Biol. Chem.* **274,** 10113–10118.
23. Tomaselli, G. F., Beuckelmann, D. J., Calkins, R. D., Berger, Kessler, P. D., Lawrence, J. H., Kass, D., Feldman, A. M. & Marban, E. (1994) *Circulation* **90,** 2534–2539.
24. Girgis, I., Gualberti, J., Langan, L., Malek, S., Mustaciuolo, V., Costantino, T. & McGinn, T. G. (1997) *Chest* **112,** 646–653.
25. Lopez, J. A., Harold, J. G., Rosenthal, M. C., Oseran, D. S., Schapira, J. N. & Peter, T. (1987) *Am. J. Cardiol.* **59,** 376–377.
26. Weiner, I., D. Rubin, A., Marinez, E., Postman, J. & Herman, M. V. (1981) *Mt. Sinai J. Med.* **48,** 53–55.
27. Collins, F. S. (1995) *Nat. Genet.* **9,** 347–350.
28. Mein, C. A., Esposito, L., Dunn, M. G., Johnson, G. C., Timms, A. E., Goy, J. V., Smith, A. N., Sebag-Montefiore, L., Merriman, M. E., Wilson, A. J., *et al.* (1998) *Nat. Genet.* **19,** 297–300.
29. Miki, Y., Swensen, J., Shattuck-Eidens, D., Futreal, P. A., Harshman, K., Tavtigian, S., Liu, Q., Cochran, C., Bennett, L. M., Ding, W., *et al.* (1994) *Science* **266,** 66–71.
30. Pratt, R. E. & Dzau, V. J. (1999) *Hypertension* **33,** 238–247.
31. Cooper, D. N., Smith, B. A., Cooke, H. J., Niemann, S. & Schmidtke, J. (1985) *Hum. Genet.* **69,** 201–205.
32. Wang, D. G., Fan, J. B., Siao, C. J., Berno, A., Young, P., Sapolsky, R., Ghandour, G., Perkins, N., Winchester, E., Spencer, J., *et al.* (1998) *Science* **280,** 1077–1082.
33. Collins, F. S., Guyer, M. S. & Charkravarti, A. (1997) *Science* **278,** 1580–1581.